Ultrafast dynamics in 2,6-Dimethylpyridine investigated by sub-20-fs resolved UV pump - XUV probe photoelectron spectroscopy

MASTER DEGREE IN ENGINEERING PHYSICS

Author: EDOARDO ALBERTO BOATI

Advisor: MAURO NISOLI

Co-advisors: MAURIZIO BATTISTA REDUZZI, STEFANO SEVERINO

Academic year: 2023-2024

1. Introduction

Over the past two decades, intense interest has centered on investigating the dynamics of molecules at the electron's characteristic time scale, preceding substantial nuclear motion. Notably, the exploration of molecules like pyridine and its derivatives, has driven a lot of interest caused by their crucial roles in areas such as UV photodamage of nucleic acids or more generally in biological systems. The *time-resolved photoelectron spectroscopy* TRPES represents one of the most interesting technologies in the attosecond science, it allows to visualize and control the electron motion in molecules opening the possibility for the ultimate real-time control of chemical reactions. As attosecond technologies emerged, characterizing ultrafast pulses became imperative, leading to the development of systems like RABBITT and attosecond streak cameras.

This study delves into understanding the impact of substituents, in particular by 2,6-dimethylpyridine, which showcases how they can profoundly alter molecular dynamics post UV excitation. The research employs a pump UV and probe XUV experiment to explore this specific case. Regarding the tools exploited for the study, the present work focuses on the temporal reconstruction of XUV and UV pulses using the STRIPE algorithm [2].

The thesis contains the results of the work from pulse reconstruction to utilizing these pulses for studying the biologically significant 2,6-dimethylpyridine, offering insights into the fundamental steps involved in conducting attosecond experiments [1].

2. Theory of Attosecond Physics

In this section some crucial aspect on the theory behind this field are outlined.

2.1. HHG

HHG is a fundamental process when dealing with attosecond physics and technologies, since it allows the generation of extreme ultraviolet XUV pulses. It requires the focusing of a laser pulse into a focal region (intensities of about $10^{13} - 10^{15}$ W/cm^2) filled with gas, typically a noble gas. The odd harmonics of the fundamental radiation can be generated with an efficiency that follows a trend with a plateau and a cut-off.

2.2. Attosecond Pulses Characterization

Two of the main methods to characterize attosecond pulses are the attosecond streak camera and RABBITT.

The general principle of these techniques can be summarised in an experiment which purpose is to map the pulse we want to measure in the photoelectron wave function. The electron wavefunction will encode the information about the pulse. Generally the procedure involves a two colours photionization and by varying the delay between the two different colour pulses one can obtain information about the temporal structure of the attosecond pulse and other characteristics like the chirp.

3. Experimental Setup

Here the UV pump XUV probe beamline with sub-20 fs temporal resolution is presented. UV pulses centered at 268 nm with μJ level energy are generated by frequency up-conversion between sub-10 fs visible/IR pulses generated by the hollow-core fiber compression technique and narrow-band pulses at 400 nm in a 20-μm Type-I BBO crystal. The XUV pulses are generated by selecting a single harmonic of the spectrum obtained via HHG, through a time-delay compensated monochromator (TDCM) [3]. The characterization of the pulses provided us a XUV duration of 5 fs and a UV duration of 15 fs.
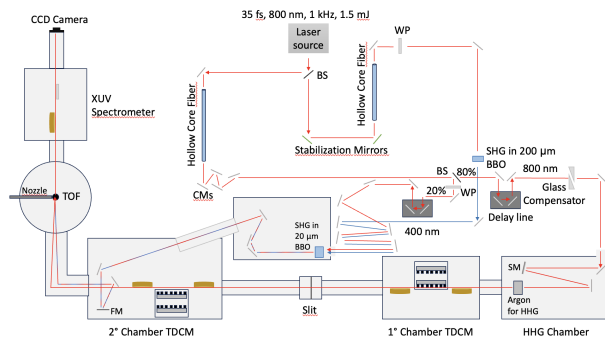

Figure 1: Simplified scheme of the complete experimental setup.

4. XUV and UV Pulse Reconstruction

In our pump and probe spectroscopy experiments we exploit the 25th harmonic of the fundamental at 800 nm, therefore there is no inter-

est in reconstructing the relative phase between the different generated harmonics. This reason brought us to use an approach called Simplified Trace Reconstruction In the Perturbative regimE STRIPE, typically much faster than the other ones currently known. The XUV pulse works as a pump, so it produces photoelectron out of argon atoms, subsequently they are probe by the UV pulses. This creates two different interference signals called sidebands. The energy of these signals will be centered at the kinetic energy of the photoelectrons determined by the energy of the XUV pulse and the ionization potential of the argon plus (in case of UV photon emission by the electron) or minus (in case of UV photon absorption by the electron) the UV photon energy as reported in fig.2.
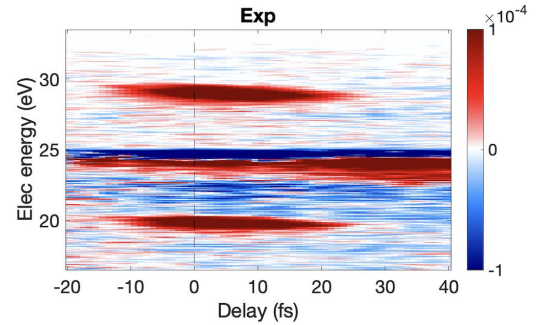

Figure 2: Experimental photoelectron trace with the sideband signals. The electron energy axis represents the kinetic energy of the electron when detected, the other is the delay between the XUV and UV pulses.

4.1. Data

The required input data for the temporal pulses reconstruction through STRIPE are the following: spectra of the XUV and UV pulses, XUV-UV photoelectron trace (PON - pump on), XUV only photoelectron trace (POF- pump off).

The STRIPE model is based on some approximation [2] which allow to define a simplified formula for the signal:

$$S(\omega,\tau) \cong \left| \int_{+\infty}^{-\infty} dt \, E_{XUV}(t+\tau) \, e^{i\frac{p_c}{\omega_0^2}E_{UV}(t)} e^{i\omega t} \right|^2 \quad (1)$$

Lastly, the STRIPE algorithm requires some initial guesses to perform a nonlinear least-squares curve fitting as implemented in MATLAB.

4.2.   Results

The best reconstruction was found after various attempts. In fig.3 it is reported the experimental positive sideband.
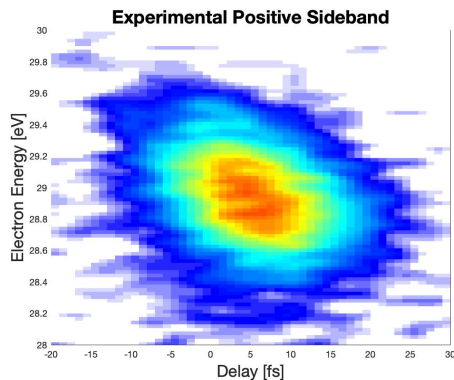

Figure 3: Experimental reference positive sideband. The electron energy axis represents the kinetic energy of the electron when detected, the other one is the delay between the XUV and UV pulses.

In fig.4 it is showed the reconstructed positive sideband with STRIPE.
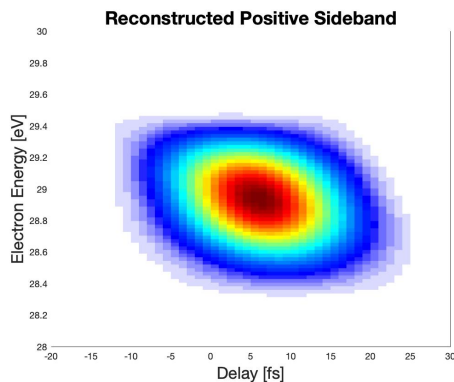

Figure 4: Reconstructed positive sideband with STRIPE algorithm. The electron energy axis represents the kinetic energy of the electron when detected, the other one is the delay between the XUV and UV pulses.

The quality of the reconstruction can be checked through various parameters and methods. The sum along the delay axis for the energy centering and the sum on the energy axis for the delay centering both provided very good results compared with the experimental data. Eventually the tilt of the sidebands was computed and compared to the experimental one, both for the negative and the positive one. In the second case the the an-

gular coefficient of the linear fit for the tilt of the center of mass is equal to -0.0075 for the experimental one and -0.0069 for the reconstructed case. This gives a relative error of 7.6%. In the negative case the experimental angular coefficient is -0.0082 and the reconstructed one -0.0072, so a relative error of 12%.

Eventually the computed XUV and UV pulses in the time domain are shown in fig.5, providing a value for the FWHM of 6 fs for the XUV and 15 fs for the UV.
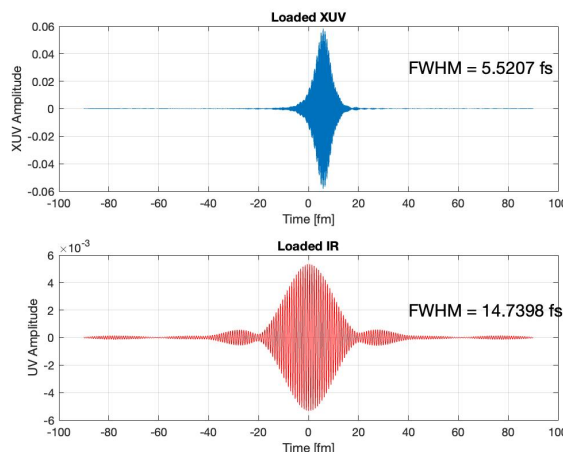

Figure 5: Reconstructed XUV and UV pulses in the time domain.

5.   Pump   and   Probe   Spectroscopy   on   2,6- Dimethylpyridine

In this section the results on the pump and probe spectroscopy experiments on 2,6-dimethylpyridine (fig.6) are presented.
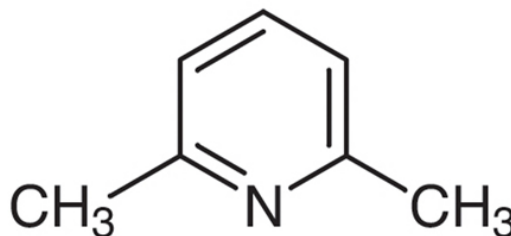

Figure 6:   Molecular structure of 2,6-dimethylpyridine.

5.1.   Pyridines

Photoexcited polyatomic molecules frequently exhibit quite complex dynamics involving the redistribution of both charge and energy. Their

dynamics is often dominated by non-adiabatic coupling of vibrational and electronic degrees of freedom, therefore they are described outside the Born-Oppenheimer approximation. These dynamics can bring the molecules into intermediate structures formed through radiationless transitions called *dark* structures.

Pyridine C_5H_5N does not represent an exception and is subject to the dynamics described above. There exist derivatives of this molecule created by adding methyl groups like 2-methylpyridine and 2,6-dimethylpyridine. These molecules become interesting when we consider the fact that modifications in the structure of the pyridine could result in a change of its behaviour once it is photoexcited. In this work the 2,6-dimethylpyridine behaviour is explored.

5.2. Methodology

As mentioned before, pump and probe spectroscopy experiments were performed. This technique involves a first pulse (pump), which drives the system out of equilibrium, and a second pulse (probe), which follows the dynamics initiated by the pump. In this work a UV pump centered around 270 nm and a XUV probe centered around 38.75 eV were exploited for the experiment; a TOF (time of flight) spectrometer was employed to measure the energy of the photoelectrons.

5.3. Data

Two different kinds of photoelectron traces were collected. The first can be labelled as *High Resolution Scans* HS and is characterized by a smaller delay axis range explored between the UV and the XUV pulses with a resolution of 5 fs. The other one presents a wider delay axis range with a step of 25 fs between one point and the next one, those are called *Low Resolution Scans* LS. The collection of two different kind of scans allows to recognize and study different dynamics, for instance the HS allows the observation of processes with shorter characteristic times, while a wider range of delays in the LS can contain an interesting evolution which could require even hundreds of fs to take place. Pre-processing on the data was performed as well. Both in the case of HS and LS, various scans were collected in different days and this made impossible to have the exact same condi-

tions each day. The first essential step is the calibration of the energy axis in the traces through a reference spectrum. In particular, the binding energy axis is defined as the difference between the XUV photon energy and the kinetic energy of the photoelectron. Once the calibration is completed the energy axes of different traces have to be centered both in delay and energy axis, since they could be decentered especially if coming from different days. This procedure was made by identifying a feature in the photoelectron trace and use it as a feature to align all the traces.

5.4. 2,6-dimethylpyridine High Resolution Scan

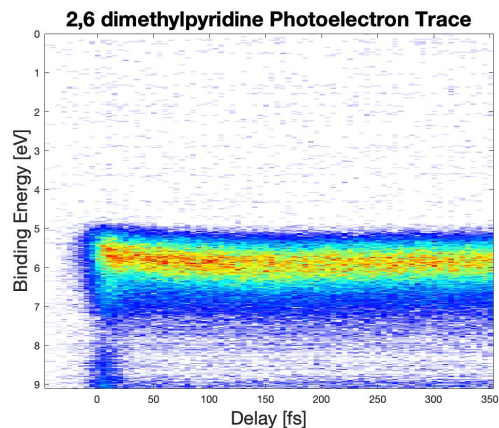The photoelectron trace is reported in fig.7.

Figure 7: Photoelectron trace of 2,6-dimethylpyridine.

The relaxation process is not immediately clear from the figure, however a deeper analysis shows this kind of dynamic. The signal center of mass of the energy CM provides a clear relaxation pattern as reported in fig.8 within the first 150 fs with an energy variation of about 0.15 eV and a rise immediately after. A deeper analysis provides a characteristic time of the decay and the rise of about 160 fs. As explained in section 5.1, the decay processes can be attributed to different physical phenomena. In particular the ring opening reaction, within this framework, is a documented evolution for pyridine and 2-methylpyridine [4]. The case of 2,6 dimethylpyridine allows to understand the important role of the methyl group. Upon methyl substitution, the electron-donating nature of these groups increases the electron den-

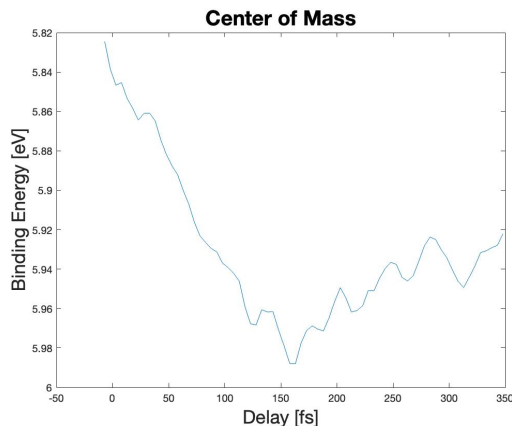sity on the ring, leading to greater stability.

Figure 8: Energy center of mass of 2,6-dimethylpyridine signal.

This stabilization in the case of 2-methylpyridine is not great enough to prevent a significant change in the structure as the ring opening reaction after the UV excitation. However the two methyl groups further enhance the stabilization, in particular 2,6-dimethylpyridine undergoes a *hot transition* which means a transition between two excited vibrational states of the molecule [4]. This implies that normal mode of the molecule can be excited by this transition and therefore observed, so the focus was shifted to the oscillations in the photoelectron trace.

Two different kind of oscillations after the delay value of 110 fs were studied: those of the intensity of the signal in the photoelctron trace and those of the CM.
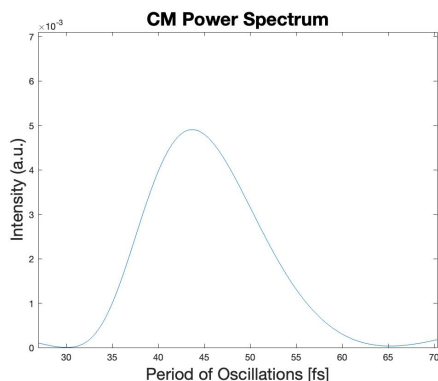

Figure 9: Power Spectrum of CM oscillation in HS.

With Fourier analysis coherent oscillations were found in both cases and the power spectrum shows periods of about 48 fs in both the cases,

the CM case is reported in fig.9. It is important to notice that such periods would be difficult to distinguish from the noise in the case of LS, since they have a resolution of 25 fs.

5.5. 2,6-dimethylpyridine Low Resolution Scan

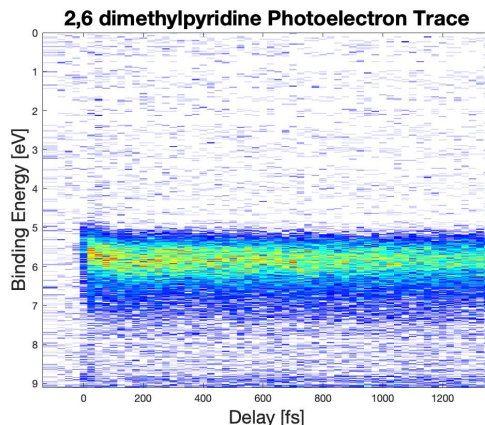The photoelectron trace is reported in fig.10.

Figure 10: Photoelectron trace of 2,6-dimethylpyridine for LS.

The CM of the signal is computed as in the case of the HS and shown in fig.11. It emerges the same variation of energy in the first 200 fs of the delay. However in this case the resolution is lower and analysis as precise as the one made with the HS is not possible.
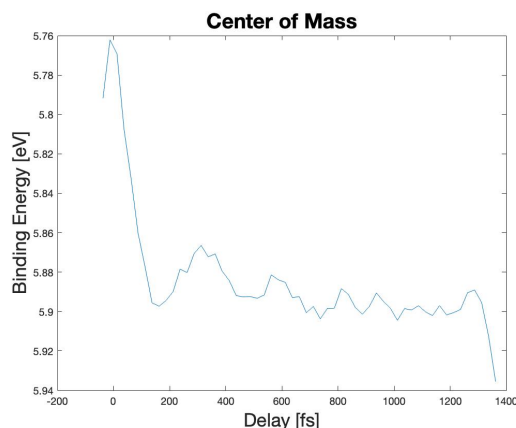

Figure 11: Energy center of mass of 2,6-dimethylpyridine signal for LS.

Nonetheless it is possible to study the first decay of the CM. A fit was performed from which two values were computed. The characteristic time of the first, higher signal within the 200 fs

in fig.11 was estimated as the FWHM of a fitted gaussian, providing a value of 120 fs. It represents the initial relaxation after the UV excitation. At longer values of the delays, it appears from fig.11 that a decay with an oscillatory nature is taking place. The characteristic time of this decay can be estimated as the characteristic time of an exponential, which provides a value of 2.5 ps. This value should be taken with caution, since the entire delay spanned only amounts to a a little more than one thousand of femtoseconds. The oscillations were analysed for the LS too, both for the intensity of the photoelectron signal and the CM. The power spectrum of the CM oscillations is reported in fig.12 showing components in the range between 250 - 300 fs which is almost equal to the whole interval in which the this kind of dynamic was studied for the HS.
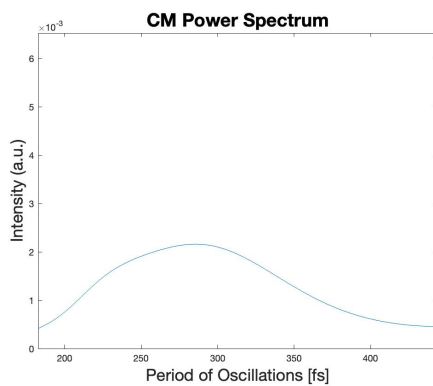

Figure 12: Power Spectrum of CM oscillation in LS.

This implies that in the HS case the longer oscillation was removed together with the baseline, the same thing is not happening for the LS where the time periods of hundreds of fs are clearly visible.

6.   Conclusions

We showed the process of temporal reconstruction of the UV and XUV pulses through the means of the STRIPE algorithm. First of all we illustrated the issues with the initial data and the problems in the reconstruction they caused which brought to change the XUV photons spectrum with a photoelectrons spectrum. Eventually the reconstruction with the new data presented a much better performance and results. The final pulses were reconstructed finding a good duration of about 5 fs and 15 fs respec-

tively for the XUV and the UV.

We showed an application of the attosecond technology, namely a UV pump XUV probe spectroscopy experiment on 2,6 dimethylpyridine. We reported the characteristic times of the relaxation process after the photoexcitation by the 268 nm UV pump of the molecule, explaining the fundamental difference in the nature of this evolution with respect to the other pyridine derivatives. In the case of the 2,6 dimethylpyridine a transition between different vibrational states is taking place, we computed and showed the coherent oscillations excited by this process. Eventually we pointed out precisely also the differences between the two kind of data represented by the SS and LS, since they provide different information on the same process, therefore showing the importance of exploiting both of them to obtain a more general picture of the phenomenon.

References

[1] Rocío Borrego-Varillas, Matteo Lucchini, and Mauro Nisoli. Attosecond spectroscopy for the investigation of ultrafast dynamics in atomic, molecular and solid-state physics. *Reports on Progress in Physics*, 85(6):066401, 2022.

[2] Bruno Moio, Fabio Medeghini, Gian Luca Dolso, Giacomo Inzani, Nicola Di Palo, Rocío Borrego-Varillas, Mauro Nisoli, and Matteo Lucchini. Reconstruction of few-fs xuv pulses with a perturbative approach. In *EPJ Web of Conferences*, volume 255, page 11008. EDP Sciences, 2021.

[3] Luca Poletto, Paolo Villoresi, Fabio Frassetto, Francesca Calegari, Federico Ferrari, Matteo Lucchini, Giuseppe Sansone, and Mauro Nisoli. Time-delay compensated monochromator for the spectral selection of extreme-ultraviolet high-order laser harmonics. *Review of Scientific Instruments*, 80(12):123109, 12 2009.

[4] Ramesh Srinivasan, Jonathan S Feenstra, Sang Tae Park, Shoujun Xu, and Ahmed H Zewail. Dark structures in molecular radiationless transitions determined by ultrafast diffraction. *Science*, 307(5709):558–563, 2005.